

Accepted Manuscript

DNA intercalators based on (1,10-phenanthrolin-2-yl)isoxazolidin-5-yl core with better growth inhibition and selectivity than cisplatin upon head and neck squamous cells carcinoma

Maria G. Varrica, Chiara Zagni, Placido G. Mineo, Giuseppe Floresta, Giulia Monciino, Venerando Pistarà, Antonio Abbadessa, Angelo Nicosia, Rogerio M. Castilho, Emanuele Amata, Antonio Rescifina

PII: S0223-5234(17)30970-4

DOI: [10.1016/j.ejmech.2017.11.067](https://doi.org/10.1016/j.ejmech.2017.11.067)

Reference: EJMECH 9942

To appear in: *European Journal of Medicinal Chemistry*

Received Date: 8 October 2017

Revised Date: 22 November 2017

Accepted Date: 24 November 2017

Please cite this article as: M.G. Varrica, C. Zagni, P.G. Mineo, G. Floresta, G. Monciino, V. Pistarà, A. Abbadessa, A. Nicosia, R.M. Castilho, E. Amata, A. Rescifina, DNA intercalators based on (1,10-phenanthrolin-2-yl)isoxazolidin-5-yl core with better growth inhibition and selectivity than cisplatin upon head and neck squamous cells carcinoma, *European Journal of Medicinal Chemistry* (2017), doi: 10.1016/j.ejmech.2017.11.067.

This is a PDF file of an unedited manuscript that has been accepted for publication. As a service to our customers we are providing this early version of the manuscript. The manuscript will undergo copyediting, typesetting, and review of the resulting proof before it is published in its final form. Please note that during the production process errors may be discovered which could affect the content, and all legal disclaimers that apply to the journal pertain.



DNA intercalators based on (1,10-phenanthrolin-2-yl)isoxazolidin-5-yl core with better growth inhibition and selectivity than cisplatin upon head and neck squamous cells carcinoma

Maria G. Varrica ^a, Chiara Zagni ^a, Placido G. Mineo ^{b-e}, Giuseppe Floresta ^{a,b}, Giulia Monciino ^a, Venerando Pistarà ^a, Antonio Abbadessa ^b, Angelo Nicosia ^b, Rogerio M. Castilho ^f, Emanuele Amata ^a, Antonio Rescifina ^{a,*}

^a Dipartimento di Scienze del Farmaco, Università degli Studi di Catania, V.le A. Doria, 95125 Catania, Italy

^b Dipartimento di Scienze Chimiche, Università di Catania; Viale A. Doria, 6; 95125- Catania, Italy.

^c CNR-IPCB Istituto per i Polimeri, Compositi e Biomateriali; Via P. Gaifami 18, I-95126 Catania, Italy

^d CNR-IPCF Istituto per i Processi Chimico-Fisici; Viale F. Stagno d'Alcontres 37, I-98158, Messina, Italy

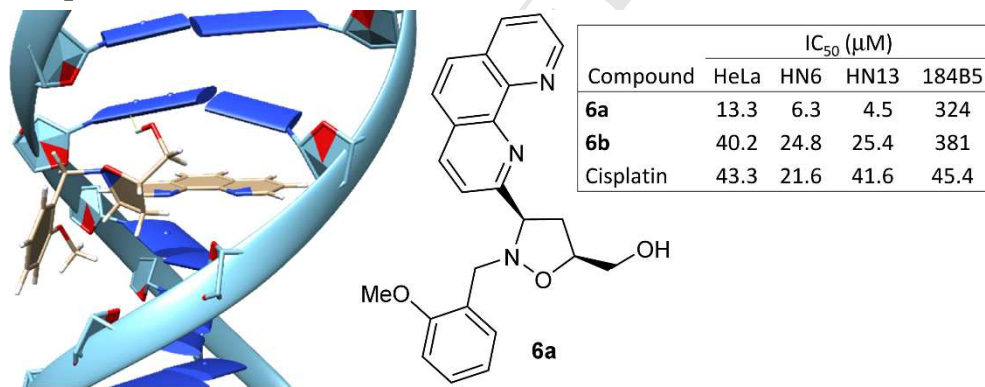
^e INSTM Consorzio Interuniversitario Nazionale per la Scienza e Tecnologia dei Materiali (UdR of Catania); Viale A. Doria, 6; I-95125, Catania, Italy

^f Laboratory of Epithelial Biology, Department of Periodontics and Oral Medicine, University of Michigan School of Dentistry, Ann Arbor, MI 48109-1078, USA

Corresponding author:

Antonio Rescifina arescifina@unict.it

Graphical Abstract



Highlights

- New 1,10-phenanthrolin-2-yl-substituted isoxazolidines have been synthesized
- The molecules act as DNA intercalators with anticancer activity
- The anticancer activity against the cisplatin-resistant HN13 cell lines was of 4.5 μM

Keywords

DNA-intercalators; 1,3-Dipolar cycloaddition; Isoxazolidines; HeLa; Head and neck squamous cells carcinoma

Abstract

((3*RS*,5*SR*)- and ((3*RS*,5*RS*)-2-(2-methoxybenzyl)-3-(1,10-phenanthrolin-2-yl)isoxazolidin-5-yl)methanol have been synthesized, according to 1,3-dipolar cycloaddition methodology, as DNA intercalating agents and evaluated for their anticancer activity against human cervical carcinoma HeLa and head and neck squamous cells carcinoma cell lines. The synthesized compounds exhibited good cytotoxic activity with IC₅₀ better than cisplatin, used as the main and effective treatment for HNSCC, and a 24.3–72.0-fold selectivity respect to the 184B5 non-cancerous immortalized breast epithelial cell lines. Unwinding assay, circular dichroism data, and Uv-vis melting experiments confirmed that these compounds act as DNA intercalators with a binding constant in the order of 10⁻⁴ M⁻¹. Docking studies showed that both compounds can interact as intercalating agent with both poly-d(AT)₂ and poly-d(GC)₂, preferring an entrance by the minor groove of the poly-d(AT)₂.

1. Introduction

The discovery of new compounds with antitumor activity is one of the most important goals in medicinal chemistry [1-4]. An important class of chemotherapeutic agents used in cancer therapy is represented by small molecules that interact with DNA. Two broad classes of noncovalent DNA-binding agents have been identified, the intercalators [5, 6] and the groove binders [7]. Intercalators are small molecules that can reversibly bind in between adjacent base pairs of double-stranded DNA (dsDNA) by inserting a planar aromatic chromophore. This process causes lengthening, stiffening and unwinding of the DNA helix. Groove binders fit into the DNA minor groove causing little perturbation of the DNA structure [8].

Representative examples of classical intercalators are acridine derivatives such as DACA [9], or acridine orange [10], dyes such as methylene blue [11], phenanthridine derivatives such ethidium bromide [12], doxorubicin [13], quinacrine [14], and actinomycin [15] (Fig. 1).

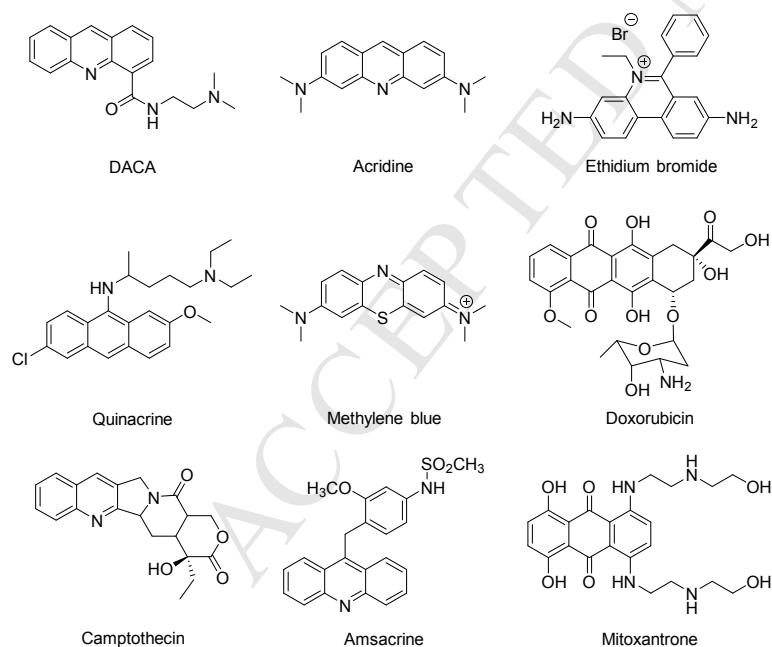


Fig. 1. Selected DNA intercalating agents and Topoisomerase inhibitors.

In 1970 a group of enzymes, called topoisomerases [16], involved in the control of the shape of DNA, was discovered. These enzymes control the topology of the supercoiled DNA double helix

during the transcription or replication of cellular genetic materials. They allow the relaxation of supercoiled DNA through a mechanism implicating the breakage of a phosphodiester bond of either one strand (Topo I) or both strands (Topo II) of the duplex DNA [17]. Among topoisomerase I poisons camptothecin and its derivatives are the best representatives [18], while topoisomerase II inhibitors examples are amsacrine and mitoxantrone [19] (Fig. 1).

Following our ongoing interest in the synthesis and biological evaluation of new DNA intercalators [20-25], here we report the synthesis and the biological activity of novel functionalized isoxazolidines where the aromatic moiety has been replaced by 1,10-phenanthroline ring [26, 27].

We reasoned that phenanthroline-isoxazolidine conjugates might provide new compounds for the development of bioactive mimics. Thus, the main focus of this paper is to design a new phenanthroline-isoxazolidines and verify whether these new hybrid agents induce antiproliferative effect, leading to cell growth perturbation.

Compounds **6** have been synthesized in good yields according to the 1,3-dipolar cycloaddition methodology [28-32], which is a chemical reaction between a 1,3-dipole and a dipolarophile to produce five-membered rings, just reported by us in an eco-friendly procedure [33]. The ability of the new compounds to intercalate into DNA and inhibit Topo I enzyme was tested *in vitro*. Moreover, the compounds were screened over three carcinoma cell lines, human cervical carcinoma (HeLa) and head and neck squamous cells carcinoma (HNSCCs), in order to test their ability to inhibit cancer cells growth. The compounds showed anticancer activity in the low micromolar range with the *cis* stereoisomer slightly more active than the *trans* one.

Finally, circular dichroism, **Uv-vis melting experiments**, and docking studies demonstrate that compounds **6** effectively intercalate between DNA base-pairs approaching the duplex from the minor groove **and quantitatively justify the observed biological results**.

2. Results and discussion

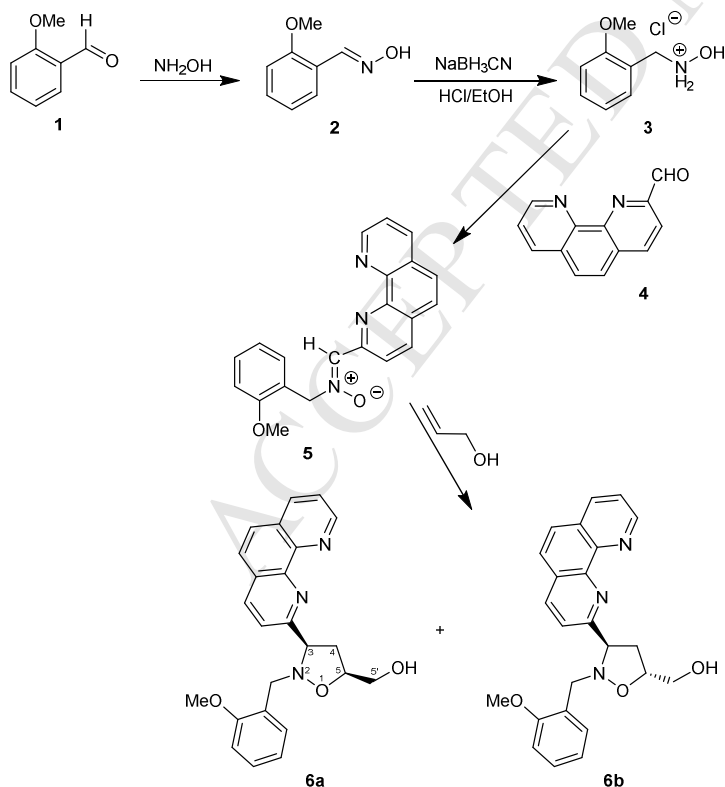
2.1. Chemistry

The strategy of the synthetic approach is based on the construction of new nitron **5**, which has been

prepared as a mixture of *Z/E* isomers (9:1), in 47% yield, by reaction of 1,10-phenanthroline-2-carbaldehyde **4** [34] and *N*-(2-methoxybenzyl)hydroxylamine **3** [35].

The ^1H NMR spectrum of crude reaction shows the presence of two diagnostic methine protons at 9.18 and 9.19 ppm indicative of the presence of *E/Z* isomers. NOE measurements allow assigning the configuration of the major compound. In particular, irradiation of the benzylic proton at 5.24 ppm induced a positive NOE effect on the downfield resonance of methine proton at 9.18 ppm representative of a *cis* relationship between these protons, thus suggesting a *Z* configuration for this nitron. On the contrary, no NOE effect was observed for the minor compounds when the benzylic proton at 5.29 ppm was irradiated.

Subsequent reaction of nitron **5** with allyl alcohol in excess at 100 °C in a sealed tube for 3 h afforded a mixture of two isoxazolidines **6** (Scheme 1). The cycloaddition reaction proceeds with high regioselectivity but low stereoselectivity giving rise only 5-substituted regioisomers in a *cis/trans* configuration and in 1:1 ratio.



Scheme 1. Synthesis of target isoxazolidine derivatives. Reagents and conditions: a) sodium acetate, CH_2Cl_2 , 30 min at 0 °C and then at room temperature overnight; b) allyl alcohol, sealed tube 100 °C for 3 h.

The structure of adducts has been elucidated by ^1H NMR and ^{13}C NMR spectroscopies and MS spectrometry. The ^1H NMR spectrum of **6** as C_5 regioisomers exhibit the diagnostic resonance of the H_5 protons at 4.34 and 4.55 ppm, while the methylene protons at C_4 resonate at 2.62–2.66 and 2.91–3.10 ppm. As regards the 4-substituted regioisomers it is known that these compounds do not show resonance at these chemical shift values.

The *cis/trans* configuration of the obtained adducts has been determined by NOE experiments. In particular, irradiation of H_5 (4.55 ppm) in compound **6a** induces a positive NOE effect on the downfield resonance of methylene proton at C_4 (H_{4b}), centered at 3.10 ppm, and on H_3 , centered at 4.75 ppm. Conversely, the irradiation of H_{4a} not induced any positive NOE effect on H_3 and H_5 protons, but produces a positive effect on H_{4b} and the hydroxymethylenic protons linked to C_5 of isoxazolidine ring. These results revealed that H_3 , H_{4b} , and H_5 are in a *cis* relationship. Irradiation of H_5 in compound **6b** induces a NOE enhancement for the downfield resonance of methylene protons at C_4 (H_{4b}) centered at 2.91 ppm; irradiation of H_3 centered at 4.81 ppm produced a positive NOE on H_{4a} , while the irradiation of H_{4a} induced a positive NOE on H_3 , H_{4b} and the hydroxymethylenic protons at C_5 . Finally, the irradiation of H_{4b} generated a positive NOE on H_5 . These data unequivocally indicate that compound **6b** is in a *trans* configuration. (Scheme 1).

2.2. Biological evaluation

2.2.1. Cytotoxicity assays

The cytotoxicity of compounds **6** was evaluated *in vitro* against HeLa and HNSCCs cell lines HN6 and HN13. As a screening assay, the cytotoxicity was tested using an MTT tetrazolium reduction assay and expressed as IC_{50} values where IC_{50} is the drug concentration causing 50% inhibition of the cell growth. Results shown in Table 1 indicates that the isoxazolidines **6** displayed good cytotoxicity against the tested cell lines. In particular, the new derivatives **6** showed a slightly improved cytotoxic activity toward HeLa cells respect to the compounds previously reported by us exhibiting IC_{50} values in the low micromolar range [22, 23]. The stereochemical configuration disclosed a low impact on the activity. In fact, the *cis* isoxazolidine **6a** was slightly more active than

the *trans* one **6b** over all the cell lines tested.

Table 1

In vitro efficacy assay of compounds **6** on selected HNSCC cell lines and on non-cancerous cells expressed as IC₅₀^a (μM) at 24 h

Compound	HeLa	HN6	HN13	184B5
6a	13.3 ±0.2	6.3 ±0.7	4.5 ±0.6	324 ±12
6b	40.2 ±1.4	24.8 ±1.1	25.4 ±1.0	381 ±17
Cisplatin	43.3 ±2.3	21.6 ±1.5	41.6 ±2.4	45.4 ±2.9

^a Mean of three independent triplicate experiments ± standard error.

Interesting, compound **6a** displayed better growth inhibition than cisplatin (3.4–9.2-fold), here chosen as reference compound because it is an established and effective treatment for HNSCC [36]; moreover, and more importantly, these cell lines are particularly resistant to cisplatin. Finally, to determine if the newly synthesized compounds have differential cytotoxic effects on cancer and non-cancer cells, their cytotoxicity was also evaluated using 184B5 non-cancerous immortalized breast epithelial cell lines. We found that the antiproliferative activity of compound **6a** was not pronounced against the non-cancerous cell lines (Table 1) with 24.3, 51.4, and 72.0-fold selectivity respect to the more resistant HeLa, HN6, and HN13 cancer cell lines, respectively.

2.2.2. Unwinding assay

DNA topoisomerases are essential enzymes that exert their important cellular roles by relaxing the superhelical tension [37]. Topoisomerase I (Topo I) topoisomerases catalyze the relaxation of supercoiled DNA by introducing transient single-stranded DNA breaks in one of the phosphodiester backbones of the duplex DNA. This results in a reversible Topo-I/DNA covalent complex followed by the reorganization and the reconnection of the damaged DNA strand.

In order to investigate the ability of compounds **6** to inhibit Topo I or effectively intercalate into DNA base pairs, we performed an agarose-gel electrophoresis experiment *ad-hoc* designed, based on the different electrophoretic mobility of supercoiled and relaxed conformations of DNA. The relaxation assay using topoisomerase I is one of the most robust approaches to evidence intercalation of small molecules into DNA [38].

Relaxed plasmid DNA (pGEM-T Easy) was incubated with Topo I enzyme alone or in the presence of the examined compound **6**. Topo I inhibitors will prevent the enzyme from changing the state of the relaxed DNA; whereas, in the presence of an intercalator, Topo I will convert the relaxed DNA into a supercoiled state. As seen in the right side of Fig. 2, relaxed pGEM-T Easy plasmid substrate was converted to negatively supercoiled molecules by treatment with Topo I in the presence of molecules **6** at a concentration of 10 nM, indicating that it acts as DNA intercalator.

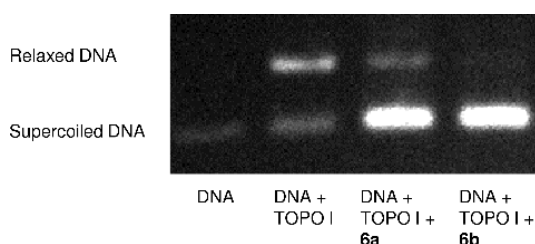


Fig. 2. Intercalation into DNA of compounds **6**. Intercalation was monitored by conversion of relaxed (R) pGEM-T Easy plasmid to negatively supercoiled molecules (SC). An agarose gel stained with ethidium bromide is shown. Control reactions were carried out in the absence of enzyme [from left to right: SC, R, compound **6a** + plasmid + Topo I, compound **6b** + plasmid + Topo I].

2.3. Circular dichroism

To gain a deeper insight into the changes of polynucleotide properties induced by **6** binding, with the aim to prove, or not, the postulated intercalation between base pairs, we studied, by circular dichroism (CD) technique, the behavior of this compound on interaction with calf-thymus DNA (ct-DNA).

The CD spectrum of ct-DNA, in B form, displays two conserved peaks at 246 and 276 nm; the first one, negative, is due to right-handed helicity whereas the second one, positive, is due to base stacking [39].

The CD titration spectra of ct-DNA, monitored in the presence of increasing amounts of **6a** were shown in Fig. 3. Increasing concentration of **6a** decreases the intensity of 276 nm signals, without any shift in its positions, and a concomitant appearance of a negative induced CD (ICD) signal at

271 nm (as a proof of the intercalation phenomenon). These results are consistent with an intercalative binding of the 1,10-phenanthroline moiety. In particular, the changes in the intrinsic CD spectrum of the ct-DNA reflect the diminished helicity (helix unwinding) and the extent of base stacking accompanied by stabilization of the right-handed B conformation of ct-DNA, as frequently observed for intercalators [40].

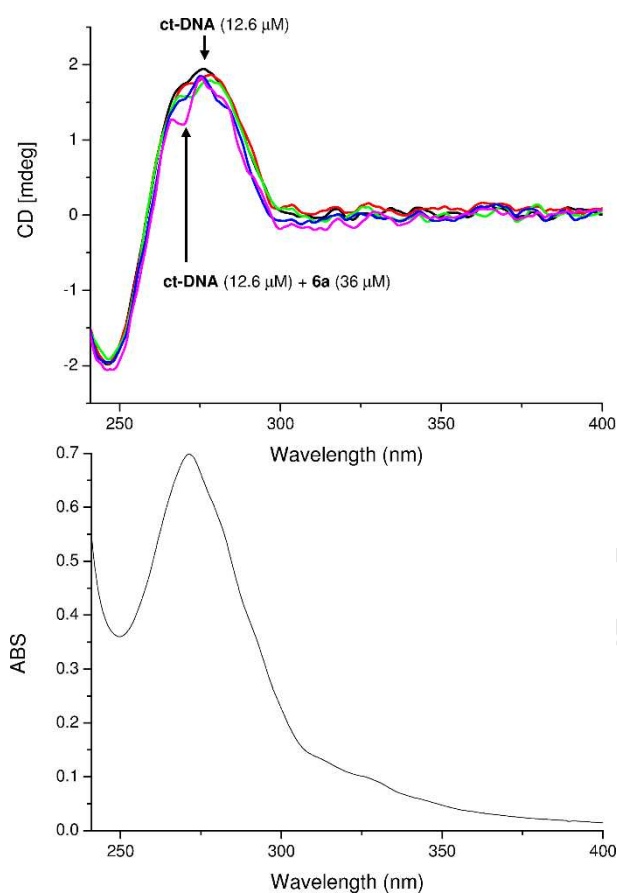


Fig. 3. CD spectra of **6a**/ct-DNA system titration at 25 °C (up) and UV-Vis spectrum of **6a** (down). **Increasing concentration of 6a decreases the intensity of the CD signal.**

The CD results of compound **6b** (Fig. 4) are similar to that of compound **6a** but without the ICD.

Finally, the small negative ICD signal at 271 nm further prove the intercalation phenomenon contemporarily establishing the geometry of ligand: the ICD sign is in accord with the pyrene moiety perpendicular to the DNA axis with its long direction almost parallel to the base-pair long axis [41, 42]. It can be noticed that, although compounds **6a** and **6b** are chiral species, they are a

racemic mixture. In fact, these systems show a silent CD spectrum, indicating that the observed ICD phenomenon is genuine.

These CD experimental data are qualitatively well in accord to those obtained *in silico* (Table 2).

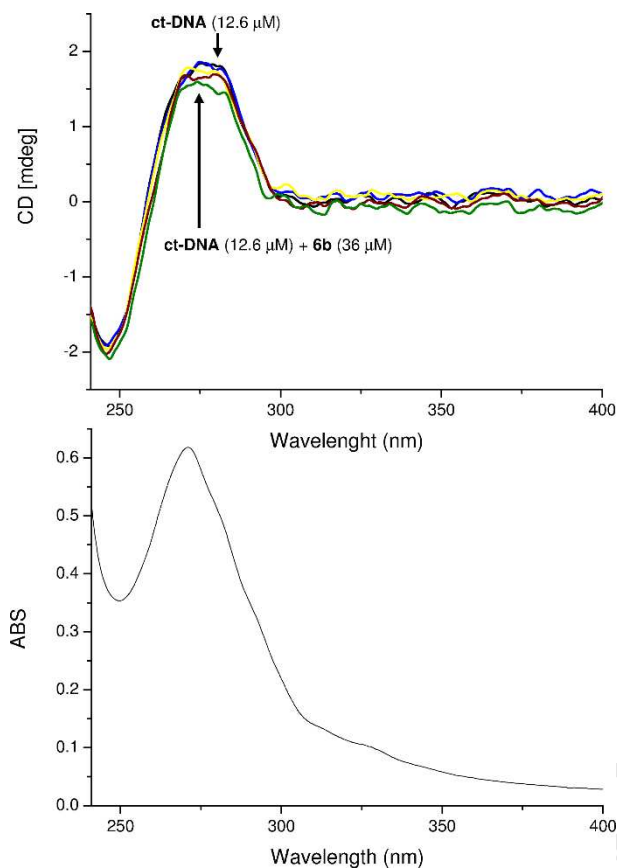


Fig. 4. CD spectra of **6b**/ct-DNA system titration at 25 °C (up) and UV-Vis spectrum of **6b** (down). Increasing concentration of **6b** decreases the intensity of the CD signal.

2.4. Evaluation of binding constants by means of ct-DNA melting experiments

To investigate the quantitative interaction between ct-DNA and compounds **6**, the thermal melting of the DNA/**6** complexes were evaluated by means of thermally controlled UV-vis experiments. In this way, because of the interactions of **6** with DNA, a variation of the melting temperature is recorded, revealing an enhancement of the ct-DNA melting temperature.

From UV-vis measurements, in absence of **6**, the melting of ct-DNA in PBS solution results 354 K, that increased at 358 K and 355 K when it is in mixture with compounds **6a** and **6b**, respectively.

From the melting temperature differences between free ct-DNA and the ct-DNA/**6** complexes (Fig. S1), using the equation 1, it is possible to calculate the binding constants of the drug molecule with ct-DNA [43].

$$\frac{1}{T_m^\circ} - \frac{1}{T_m} = \left(\frac{R}{n\Delta H_{wc}} \right) \ln(1 + KT_m\alpha) \text{ eq. 1}$$

In this equation, T_m° is the optical melting temperature of the free ct-DNA, T_m is the optical melting temperature of ct-DNA in the presence of the intercalating molecule, ΔH_{wc} is the enthalpy of ct-DNA melting, R is the gas constant, KT_m , is the drug binding constant at T_m , α is the free drug activity, and n is the site size of the drug binding. The binding constants (KT_m), calculated from the melting curves, result $4.53 \cdot 10^4 \text{ M}^{-1}$ and $9.26 \cdot 10^3 \text{ M}^{-1}$ for **6a** and **6b**, respectively.

These experimental data quantitatively parallel those obtained both *in vitro* and *in silico* (Tables 1 and 2) and, taken together with the Topoisomerase 1 and CD results, suggest that the biological activity observed for compounds **6** is effectively due to their intercalation between DNA base-pairs.

2.5. Docking studies

In order to confirm and rationalize the observed biological results and to get more insight into the intercalation modality, the supramolecular complexes of synthesized compounds with DNA have been investigated by molecular modeling methodology. Although the obtained compounds are racemates, we have already demonstrated that compounds with a 3*R* configuration possess the best intercalating properties [22]. Thus, all molecular docking calculations were performed on 3*R* stereoisomers.

For *in silico* studies, we adopted an already validated molecular modeling template consisting of three steps [23], employing, for the minimization, the AMBER14 force field including the OL15 DNA fine-tuning, that is one of the most accurate force fields widely used for proteins and DNA [44].

The possibility to achieve complexes by binding along the groove was a priori excluded according to previously reported results [21].

The obtained results showed that compound **6a** show the best intercalative properties. In particular, the inspection of Table 2 indicates that compound **6a** exhibits the highest activity, followed by **6b**, according to the biological results. Moreover, compounds **6**, in general, show a preference for the poly-AT fragment intercalating from the minor groove.

Fig. 5 reports a plot of compound **6a** intercalated into poly-d(AT)₂ from minor groove. The interaction of this compound with nucleobases involve one hydrogen bond between the hydroxylic

group of compounds **6a** and an adenine of the DNA backbone. However, other important hydrophobic and van der Waals interactions are established between the DNA and the intercalating portion of the molecule (1,10-phenanthroline ring). Particularly, this hydrogen bond is not present neither in the complex of the same molecule with poly-d(AT)₂ from the major groove nor in the complexes of **6a** with poly-d(GC)₂. Thus, we speculate that the selectivity and the potency of the molecule **6a**, respect to **6b**, is probably due to this hydrogen bond, which can be classified as a moderate, mostly electrostatic interaction.

Table 2Calculated binding energies^a for compounds **6** intercalated in d(AT)₂ and d(GC)₂ dodecamers

Compound	Poly-AT	
	From major groove	From minor groove
(3 <i>R</i> ,5 <i>S</i>)- 6a (<i>cis</i>)	-7.61	-10.01
(3 <i>R</i> ,5 <i>R</i>)- 6b (<i>trans</i>)	-7.21	-9.62
	Poly-GC	
	From major groove	From minor groove
(3 <i>R</i> ,5 <i>S</i>)- 6a (<i>cis</i>)	-7.61	-8.88
(3 <i>R</i> ,5 <i>R</i>)- 6b (<i>trans</i>)	-7.14	-7.96

^a All values are in kcal/mol.

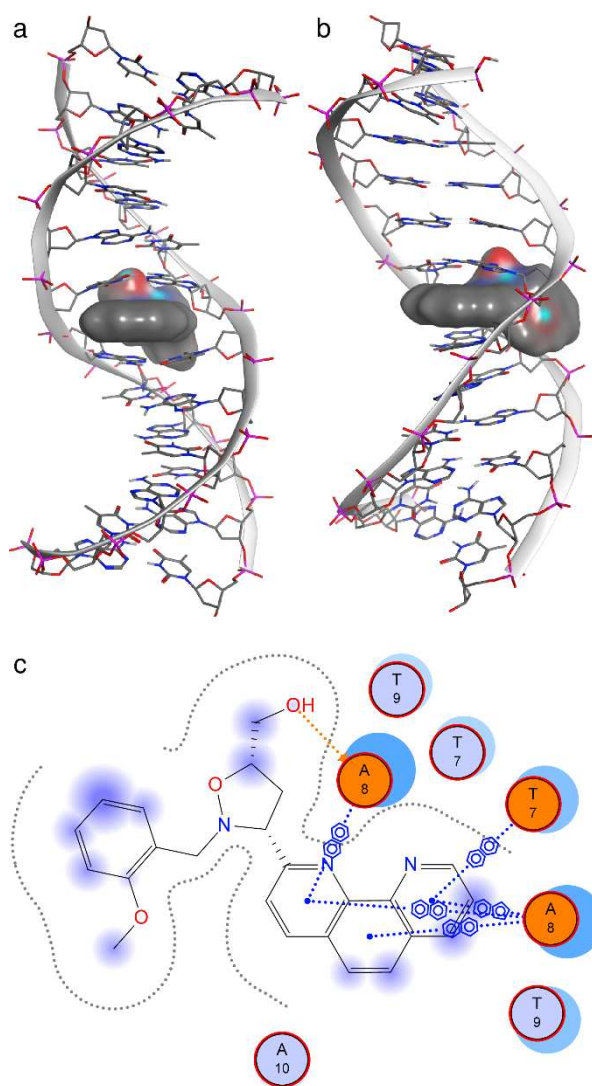


Fig. 5. Interaction of **6a** with poly-d(AT)₂ from minor groove. a) Front view, b) side view, c) 2D-interactions.

3. Conclusions

In this study, we report the synthesis and the biological properties of two novel 1,10-phenanthroline-bearing isoxazolidinyl derivatives. The obtained compounds show an interesting antitumor activity, due to DNA intercalation, over three carcinoma cell lines. All of the obtained compounds were tested for their in vitro cytotoxic activity toward three different human tumor cell lines, and the most-potent one, **6a**, showed an IC₅₀ of 4.5 μM toward the HNSCCs cell lines HN13. Moreover, compound **6a** showed a 72-fold selectivity upon the 184B5 non-cancer immortalized breast epithelial cell lines. The HNSCCs is the sixth leading cancer by incidence worldwide. Patients with HNSCCs are treated with multiple-modality therapies concerning surgery, radiation,

and chemotherapy. However, long-term survival rates in patients with advanced-stage HNSCCs have not increased significantly in the past 30 years [45, 46]. Although cisplatin is currently the most commonly used chemotherapeutic agent for HNSCCs, its administration is associated with systemic toxicities that often reduce compliance and prevent timely completion of therapy. To the best of our knowledge compound **6a** is the first intercalating agent that possesses a better growth inhibition (3.4–9.2-fold), upon cancerous HN6 and HN13 cell lines, and selectivity (24.4–65.9-fold), upon non-cancerous 184B5 cell lines, than cisplatin.

The intercalating properties, determined by electrophoresis (unwinding assay) and circular dichroism, and the estimated binding constants, calculated by Uv-vis melting point measurements, are consistent with molecular docking studies.

4. Experimental Section

4.1. Chemistry

Solvents and reagents were used as received from commercial sources. Melting points were determined with a Kofler apparatus and are reported uncorrected. Elemental analyses were performed with a Perkin–Elmer elemental analyzer. NMR spectra (^1H NMR recorded at 500 MHz, ^{13}C NMR recorded at 125 MHz) were obtained on Varian Instruments and are referenced in ppm relative to TMS or the solvent signal. Thin-layer chromatographic separations were performed on Merck silica gel 60-F254 precoated aluminum plates. Flash chromatography was accomplished on Merck silica gel (200–400 mesh). The circular dichroism spectra were recorded by means of JASCO J-815 spectropolarimeter equipped with a 150W Xenon lamp. The ellipticity was obtained calibrating the instruments with a 0.06% (w/v) aqueous solution of ammonium d-10-camphorsulfonate and with a 0.08% (w/v) aqueous solution of tris(ethylenediamine)cobalt(III) chloride complex $2\{(-)\text{-}\Delta\text{-}[\text{Co}(\text{en})_3]\text{Cl}_3\}\cdot\text{NaCl}\cdot 6\text{H}_2\text{O}$. The measurements, corrected for the contribution from cell and solvent, were performed at a constant temperature of 25 °C in quartz cells. The temperature of J-815 was controlled by means of a Jasco PTC-423S/15 Peltier-type

temperature control system cooled with an external water circulator. The spectra have been corrected to take into account the dilution effect after each addition. UV-visible spectra were recorded both at room and **variable temperature** using a Shimadzu Model 1601 spectrophotometer **equipped with a Peltier unit**, in quartz cells, using **PBS solution** as a solvent. **Compounds 2 and 4**, **although commercially available, were synthesized as reported in the literature [47, 48].**

4.1.1. Synthesis of *N*-(2-methoxybenzyl)hydroxylammonium chloride **3**

To a solution of 2-methoxybenzaldehyde oxime **2** (2.15 g, 0.014 mol) in dry CH₃OH (30 mL), containing a trace of methyl orange, NaBH₃CN (1.37 g, 21.9 mmol) was added. Subsequently, 2.5 M HCl–MeOH was added dropwise with stirring to maintain the red color of the solution for 30 min. The reaction mixture was further stirred for 4 h, and methanol was removed under vacuum to give a white solid. Yield 98%, m.p. 136–139 °C. ¹H NMR (DMSO, 500 MHz): 3.81 (s, 3H, CH₃), 4.27 (s, 2H, CH₂), 6.96–7.43 (m, 4H), 10.98 (bs, 2H, NH₂), 11.46 (bs, 1H, OH). ¹³C NMR (DMSO, 500 MHz): 48.96, 55.52, 110.95, 117.61, 120.08, 130.80, 132.07, 157.66. Anal. Calcd for C₈H₁₁NO₂•HCl: C, 50.67; H, 6.38; N, 7.39%. Found: C, 50.78; H, 6.37; N, 7.37%.

4.1.2. Synthesis of *N*-(2-methoxybenzyl)-1-(1,10-phenanthroline-2-yl)methanimine oxides **5**

To a solution of sodium acetate (0.79 g, 0.0096 mol) in dichloromethane (30 mL), cooled at 0 °C, was added the *N*-(2-methoxybenzyl)hydroxylammonium chloride **3** (1.33 g, 0.0096 mol) and successively, dropwise, the corresponding 1,10-phenanthroline-2-carbaldehyde **4** (0.67 g, 0.0032 mol). The reaction mixture was then stirred for 30 min at 0 °C and then at room temperature overnight. After this time, organic solvent was removed under reduced pressure and the obtained solid was purified by silica gel flash-chromatography (CHCl₃ saturated with ammonium hydroxide/cyclohexane 40:60) to give the pure *Z* nitron (Z)-**5**. *Z*. Yield 55%; yellow solid m.p. 198–204 °C. ¹H NMR (CDCl₃, 500 MHz): 3.87 (s, 3H), 5.24 (d, 2H, *J*=4.2 Hz), 6.94–8.32 (m, 10H), 9.18 (d, 1H, *J*=4.2 Hz), 9.51 (d, 1H, *J*=8.5 Hz). ¹³C NMR (CDCl₃, 500 MHz): 55.54, 66.50,

110.82, 120.85, 123.16, 123.25, 126.44, 127.10, 128.31, 129.42, 130.84, 132.13, 135.10, 136.28, 136.35, 136.76, 141.32, 143.45, 148.37, 150.33, 158.34. Anal. Calcd for C₂₁H₁₇N₃O₂: C, 73.45; H, 4.99; N, 12.24%. Found: C, 73.32; H, 4.97; N, 12.28%.

Further elution gave 5.5% of *E* nitron (*E*)-**5**. Yellow solid m.p. 175–180 °C. ¹H NMR (CDCl₃, 500 MHz): 3.94 (s, 3H, OCH₃), 5.29 (s, 2H, CH₂), 6.94–8.33 (m, 10H), 8.29 (s, 1H), 9.19 (s, 1H), 9.48 (d, 1H, *J*=8.5 Hz).

4.2. General procedure for the synthesis of isoxazolines **6**

A solution of nitron **5** (0.50 g, 0.012 mol) and allyl alcohol (7 mL) in a sealed tube equipped with a stir bar, was allowed to react at 100 °C for 3 h. The mixture was evaporated and the residue was purified by flash chromatography on a silica gel (CHCl₃/CH₃OH/Et₃N 98:1:1).

4.2.1. ((3*RS*,5*SR*)-2-(2-methoxybenzyl)-3-(1,10-phenanthrolin-2-yl)isoxazolidin-5-yl)methanol **6a**

Yield 44%, yellow solid. ¹H NMR (CDCl₃, 500 MHz): 2.66 (ddd, 1H, *J*=6.8, 7.7 and 14.3 Hz, H_{4a}), 3.10 (ddd, 1H, *J*=7.1, 7.9 and 14.3 Hz, H_{4b}), 3.31 (bs, 1H, OH), 3.67 (dd, 1H, *J* = 3.1 and 12.5 Hz, H_{5'a}), 3.74 (s, 3H, OMe), 3.82 (dd, 1H, *J*=4.7 and 12.5 Hz, H_{5'b}), 4.06 (d, 1H, *J*=13.5 Hz, H_{2'a}), 4.18 (d, 1H, *J*=13.5 Hz, H_{2'b}), 4.55 (dddd, 1H, *J*=3.1, 4.7, 6.8 and 7.1 Hz, H₅), 4.75 (dd, 1H, *J*=7.7 and 7.9 Hz, H₃), 6.79–7.19 (m, 4H), 7.48–8.25 (m, 6H), 9.22 (dd, 1H, *J* = 1.2 and 4.1 Hz, H₉). ¹³C NMR (CDCl₃, 125 MHz): 38.30, 54.92, 55.23, 64.86, 71.95, 77.70, 110.21, 120.40, 121.46, 122.89, 125.64, 126.25, 126.42, 127.90, 128.37, 128.83, 130.29, 136.15, 136.82, 145.30, 150.37, 155.23, 157.33, 161.27. Anal. Calcd for C₂₄H₂₃N₃O₃: C, 71.80; H, 5.77; N, 10.47%. Found: C, 71.99; H, 5.76; N, 10.49%.

4.2.2. ((3*RS*,5*RS*)-2-(2-methoxybenzyl)-3-(1,10-phenanthrolin-2-yl)isoxazolidin-5-yl)methanol **6b**

Yield 35%, yellow solid. ¹H NMR (CDCl₃, 500 MHz): 2.62 (ddd, 1H, *J*=6.8, 7.7 and 14.3 Hz, H_{4a}), 2.91 (ddd, 1H, *J* = 7.1, 7.9 and 14.3 Hz, H_{4b}), 3.27 (bs, 1H, OH), 3.63 (dd, 1H, *J* = 3.1 and 12.5 Hz,

H_{5'a}), 3.71 (s, 3H, OMe), 3.88 (dd, 1H, $J = 4.7$ and 12.5 Hz, H_{5'b}), 4.12 (s, 2H, H_{2'}), 4.34 (dddd, 1H, $J = 3.1, 4.7, 6.8$ and 7.1 Hz, H₅), 4.81 (dd, 1H, $J = 7.7$ and 7.9 Hz, H₃), 6.79–7.19 (m, 4H), 7.48–8.25 (m, 6H), 9.24 (dd, 1H, $J = 1.2$ and 4.1 Hz, H₉). ¹³C NMR (CDCl₃, 125 MHz): 38.94, 55.28, 55.69, 63.55, 72.05, 78.51, 110.28, 120.53, 121.37, 122.89, 125.84, 126.23, 126.50, 128.33, 128.88, 130.03, 130.63, 136.16, 136.81, 145.87, 148.02, 150.88, 157.12, 161.79. Anal. Calcd for C₂₄H₂₃N₃O₃: C, 71.80; H, 5.77; N, 10.47%. Found: C, 71.66; H, 5.78; N, 10.44%.

4.3. Biology

4.3.1. Cell viability assay

HN6, HN13, HeLa, and 184B5 cell viability was measured using a commercial MTT assay (CellTiter 96 Aqueous One Solution Assay, Promega Co., USA), according to the Manufacturer's instructions. The assay is based on the ability of viable cells to metabolize yellow 3-(4,5-dimethylthiazol-2-yl)-2,5-diphenyltetrazolium bromide to violet formazan that can be detected spectrophotometrically. Cells were seeded in 96-well plates at a density of 1×10^4 cells per well in complete medium containing 10% fetal bovine serum and antibiotics and incubated in 5% CO₂ and maintained in a 5% CO₂, 95% humidity atmosphere at 37 °C. Subsequent, cells were washed with serum-free medium and subsequently incubated for 24 h after treatment with test compounds. Successively, 20 μL of fresh MTT solution (5 mg/mL) was added to each well and incubated with cells at 37 °C for additional 4 h. The supernatant was removed and 100 μL of DMSO was added to each well to dissolve the formazan crystals formed by the cellular reduction of MTT. The absorbance values of each well were measured by a plate reader at a test wavelength of 490 nm. The assays were performed in triplicate and a non-linear regression analysis was used to get dose-response curves.

4.3.2. DNA unwinding assay

The assay was carried out using negatively supercoiled or relaxed pGEM-T Easy plasmid. Relaxed

plasmid was generated by treating negatively supercoiled pGEM-T Easy with Topo I. Reaction mixtures (10 mL final volume) containing 0.3 mg of supercoiled or relaxed pGEM-T Easy, Topo I and the studied compounds **6** at concentration of 10 nM were incubated in reaction buffer (50 mM Tris-HCl pH 7.5, 20 mM KCl, 1 mM EDTA, 1 mM dithiothreitol, and BSA at 0.3 mg/mL) for 30 min at 37 °C. The reactions were terminated by the addition of 0.5% SDS and 0.5 mg/mL proteinase K. Samples were incubated for 30 min at 50°C. Next, 1.2 mL of 10X loading buffer (20% Ficol 400; 0.1 M EDTA, pH 8.0, 1.0% SDS, and 0.25% bromphenol blue) were added and the reactions mixtures loaded onto a 1% agarose gel made in 1X TBE buffer. The gel was run in 1X TBE containing 0.1% SDS. After electrophoresis, DNA bands were stained with ethidium bromide (10 mg/mL) and visualized by transillumination with ultraviolet light (300 nm).

4.3.3. CD Titration

CD spectra were acquired in a standard quartz cell of 1 cm path length in the 240–400 nm range. For each spectrum, 5 runs were averaged with a 5 min equilibration interval before each scan. All the spectra were recorded using fixed concentration of ct-DNA (12.6 μ M in base pair) in the absence or in presence of different concentrations of **6a** or **6b** (4.26 mM solution in DMSO) ranging from 0 to about 35 μ M.

4.3.4. ct-DNA melting experiments

The ct-DNA and DNA/**6** complexes melting curves were obtained in the range 308–388 K. The ct-DNA sample (31 μ M in base pair) was mixed with 31 μ M (saturating drug concentrations) of **6a** or **6b** in PBS solution. The temperature of the Peltier was raised from 308 to 388 K with a heating rate of 1 K/min and monitoring the absorbance change at 260 nm [49, 50]. Melting point was obtained from the mid-point of the melting curve.

4.3.5. Molecular modeling studies

All poly-d(AT)₂ and poly-d(GC)₂ fragments were 3'- and 5'-end-capped with a phosphate group and the system configured as a fully anionic oligonucleotide. Subsequently, the geometry was fully minimized, using Yasara software (ver. 17.4.17) [51] with a convergence criterion of 0.005 kcal/mol per Å, assigning a distance-dependent dielectric of 1.0, 1–4 scale factors of 0.833 for the electrostatic part and of 0.5 for the van der Waals one, and the nonbonded cutoff on 8 Å.

Docking was performed using AutoDock 4.2.5.1 [52] using the default docking parameters, the point charges were initially assigned according to the AMBER14 force field and then damped to mimic the less polar Gasteiger charges used to optimize the AutoDock scoring function. The setup was done with the YASARA molecular modeling program.

References

- [1] R. Martinez, L. Chacon-Garcia, The search of DNA-intercalators as antitumoral drugs: what it worked and what did not work, *Curr. Med. Chem.*, 12 (2005) 127-151.
- [2] G. Pastuch-Gawolek, K. Malarz, A. Mrozek-Wilczkiewicz, M. Musiol, M. Serda, B. Czaplinska, R. Musiol, Small molecule glycoconjugates with anticancer activity, *Eur. J. Med. Chem.*, 112 (2016) 130-144.
- [3] R. Pignatello, V. Panto, L. Basile, G. Impallomeni, A. Ballistreri, V. Pistara, E.F. Craparo, G. Puglisi, New Amphiphilic Conjugates of Mono- and Bis(carboxy)-PEG(2,000) Polymers with Lipoamino Acids as Surface Modifiers of Colloidal Drug Carriers, *Macromol. Chem. Phys.*, 211 (2010) 1148-1156.
- [4] Y. Gou, J. Wang, S. Chen, Z. Zhang, Y. Zhang, W. Zhang, F. Yang, alpha-N-heterocyclic thiosemicarbazone Fe(III) complex: Characterization of its antitumor activity and identification of anticancer mechanism, *Eur. J. Med. Chem.*, 123 (2016) 354-364.
- [5] A. Rescifina, C. Zagni, M.G. Varrica, V. Pistarà, A. Corsaro, Recent advances in small organic molecules as DNA intercalating agents: synthesis, activity, and modeling, *Eur. J. Med. Chem.*, 74 (2014) 95-115.

- [6] Y. Cheng, S.R. Avula, W.W. Gao, D. Addla, V.K.R. Tangadanchu, L. Zhang, J.M. Lin, C.H. Zhou, Multi-targeting exploration of new 2-aminothiazolyl quinolones: Synthesis, antimicrobial evaluation, interaction with DNA, combination with topoisomerase IV and penetrability into cells, *Eur. J. Med. Chem.*, 124 (2016) 935-945.
- [7] A. Ali, S. Bhattacharya, DNA binders in clinical trials and chemotherapy, *Bioorg. Med. Chem.*, 22 (2014) 4506-4521.
- [8] L.S. Lerman, Structural considerations in the interaction of DNA and acridines, *J. Mol. Biol.*, 3 (1961) 18-30.
- [9] B.C. Baguley, L.P. Wakelin, J.D. Jacintho, P. Kovacic, Mechanisms of action of DNA intercalating acridine-based drugs: how important are contributions from electron transfer and oxidative stress?, *Curr. Med. Chem.*, 10 (2003) 2643-2649.
- [10] R.W. Armstrong, T. Kurucsev, U.P. Strauss, The interaction between acridine dyes and deoxyribonucleic acid, *J. Am. Chem. Soc.*, 92 (1970) 3174-3181.
- [11] E. Tuite, B. Norden, Sequence-Specific Interactions of Methylene-Blue with Polynucleotides and DNA - a Spectroscopic Study, *J. Am. Chem. Soc.*, 116 (1994) 7548-7556.
- [12] J.B. LePecq, C. Paoletti, A fluorescent complex between ethidium bromide and nucleic acids. Physical-chemical characterization, *J. Mol. Biol.*, 27 (1967) 87-106.
- [13] R.H. Blum, S.K. Carter, Adriamycin. A new anticancer drug with significant clinical activity, *Ann. Intern. Med.*, 80 (1974) 249-259.
- [14] K. Van Dyke, C. Lantz, C. Szustkiewicz, Quinacrine: mechanisms of antimalarial action, *Science*, 169 (1970) 492-493.
- [15] W. Muller, D.M. Crothers, Studies of the binding of actinomycin and related compounds to DNA, *J. Mol. Biol.*, 35 (1968) 251-290.
- [16] N. Kresge, R.D. Simoni, R.L. Hill, Unwinding the DNA topoisomerase story: The work of James C. Wang, *J. Biol. Chem.*, 282 (2007).

- [17] M.R. Webb, S.E. Ebeler, Comparative analysis of topoisomerase IB inhibition and DNA intercalation by flavonoids and similar compounds: structural determinates of activity, *Biochem. J.*, 384 (2004) 527-541.
- [18] Y.H. Hsiang, L.F. Liu, M.E. Wall, M.C. Wani, A.W. Nicholas, G. Manikumar, S. Kirschenbaum, R. Silber, M. Potmesil, DNA topoisomerase I-mediated DNA cleavage and cytotoxicity of camptothecin analogues, *Cancer Res.*, 49 (1989) 4385-4389.
- [19] D. Martincic, K.R. Hande, Topoisomerase II inhibitors, *Cancer Chemother. Biol. Response Modif.*, 22 (2005) 101-121.
- [20] A. Rescifina, M.A. Chiacchio, A. Corsaro, E. De Clercq, D. Iannazzo, A. Mastino, A. Piperno, G. Romeo, R. Romeo, V. Valveri, Synthesis and biological activity of isoxazolidinyl polycyclic aromatic hydrocarbons: potential DNA intercalators, *J. Med. Chem.*, 49 (2006) 709-715.
- [21] A. Rescifina, U. Chiacchio, A. Piperno, S. Sortino, Binding of a non-ionic pyrenylisoxazolidine derivative to double-stranded polynucleotides: spectroscopic and molecular modelling studies, *New J. Chem.*, 30 (2006) 554-561.
- [22] A. Rescifina, U. Chiacchio, A. Corsaro, A. Piperno, R. Romeo, Isoxazolidinyl polycyclic aromatic hydrocarbons as DNA-intercalating antitumor agents, *Eur. J. Med. Chem.*, 46 (2011) 129-136.
- [23] A. Rescifina, M.G. Varrica, C. Carnovale, G. Romeo, U. Chiacchio, Novel isoxazole polycyclic aromatic hydrocarbons as DNA-intercalating agents, *Eur. J. Med. Chem.*, 51 (2012) 163-173.
- [24] A. Rescifina, C. Zagni, G. Romeo, S. Sortino, Synthesis and biological activity of novel bifunctional isoxazolidinyl polycyclic aromatic hydrocarbons, *Bioorg. Med. Chem.*, 20 (2012) 4978-4984.
- [25] A. Rescifina, C. Zagni, P.G. Mineo, S.V. Giofre, U. Chiacchio, S. Tommasone, C. Talotta, C. Gaeta, P. Neri, DNA Recognition with Polycyclic-Aromatic-Hydrocarbon-Presenting Calixarene Conjugates, *Eur. J. Org. Chem.*, (2014) 7605-7613.

- [26] A. Gil, M. Melle-Franco, V. Branchadell, M.J. Calhorda, How the intercalation of phenanthroline affects the structure, energetics, and bond properties of DNA base pairs: theoretical study applied to adenine-thymine and guanine-cytosine tetramers, *J. Chem. Theory Comput.*, 11 (2015) 2714-2728.
- [27] A. Gil, V. Branchadell, M.J. Calhorda, A theoretical study of methylation and CH/ π interactions in DNA intercalation: methylated 1,10-phenanthroline in adenine-thymine base pairs, *RSC Adv.*, 6 (2016) 85891-85902.
- [28] V. Pistrà, A. Rescifina, F. Punzo, G. Greco, V. Barbera, A. Corsaro, Design, Synthesis, Molecular Docking and Crystal Structure Prediction of New Azasugar Analogues of α -Glucosidase Inhibitors, *Eur. J. Org. Chem.*, (2011) 7278-7287.
- [29] A. Corsaro, V. Pistrà, M.A. Chiacchio, E. Vittorino, R. Romeo, Synthesis of 4'-thionucleosides by 1,3-dipolar cycloadditions of the simplest thiocarbonyl ylide with alkenes bearing electron-withdrawing groups, *Tetrahedron Lett.*, 48 (2007) 4915-4918.
- [30] U. Chiacchio, G. Buemi, F. Casuscelli, A. Procopio, A. Rescifina, R. Romeo, Stereoselective Synthesis of Fused Gamma-Lactams by Intramolecular Nitrene Cycloaddition, *Tetrahedron*, 50 (1994) 5503-5514.
- [31] U. Chiacchio, D. Iannazzo, A. Piperno, R. Romeo, G. Romeo, A. Rescifina, M. Saglimbeni, Synthesis and biological evaluation of phosphonated carbocyclic 2-oxa-3'-aza-nucleosides, *Bioorg. Med. Chem.*, 14 (2006) 955-959.
- [32] U. Chiacchio, L. Borrello, L. Crispino, A. Rescifina, P. Merino, B. Macchi, E. Balestrieri, A. Mastino, A. Piperno, G. Romeo, Stereoselective Synthesis and Biological Evaluations of Novel 3'-Deoxy-4'-azaribonucleosides as Inhibitors of Hepatitis C Virus RNA Replication, *J. Med. Chem.*, 52 (2009) 4054-4057.
- [33] G. Floresta, C. Talotta, C. Gaeta, M. De Rosa, U. Chiacchio, P. Neri, A. Rescifina, gamma-Cyclodextrin as a Catalyst for the Synthesis of 2-Methyl-3,5-diarylisoxazolidines in Water, *J. Org. Chem.*, 82 (2017) 4631-4639.

- [34] F.H. Li, G.H. Zhao, H.X. Wu, H. Lin, X.X. Wu, S.R. Zhu, H.K. Lin, Synthesis, characterization and biological activity of lanthanum(III) complexes containing 2-methylene-1,10-phenanthroline units bridged by aliphatic diamines, *J. Inorg. Biochem.*, 100 (2006) 36-43.
- [35] H. Maskill, W.P. Jencks, Solvolysis of benzylazoxy tosylate and the effect of added bases and nucleophiles in aqueous trifluoroethanol and aqueous acetonitrile, *J. Am. Chem. Soc.*, 109 (1987) 2062-2070.
- [36] K.P. Pendleton, J.R. Grandis, Cisplatin-Based Chemotherapy Options for Recurrent and/or Metastatic Squamous Cell Cancer of the Head and Neck, *Clinical Medicine Insights: Therapeutics*, 5 (2013) 103-116.
- [37] J.J. Champoux, Evidence for an intermediate with a single-strand break in the reaction catalyzed by the DNA untwisting enzyme, *Proc. Natl. Acad. Sci. U. S. A.*, 73 (1976) 3488-3491.
- [38] M.R. Webb, S.E. Ebeler, A gel electrophoresis assay for the simultaneous determination of topoisomerase I inhibition and DNA intercalation, *Anal. Biochem.*, 321 (2003) 22-30.
- [39] V.I. Ivanov, L.E. Minchenkova, A.K. Schyolkina, A.I. Poletayev, Different conformations of double-stranded nucleic acid in solution as revealed by circular dichroism, *Biopolymers*, 12 (1973) 89-110.
- [40] L.D. Willimas, M. Egli, Q. Gao, A. Rich, DNA intercalation: helix unwinding and neighbor-exclusion, in, Adenine Press, 1992, pp. 107-125.
- [41] R. Lyng, T. Hard, B. Norden, Induced Cd of DNA Intercalators - Electric-Dipole Allowed Transitions, *Biopolymers*, 26 (1987) 1327-1345.
- [42] E. Grueso, R. Prado-Gotor, Thermodynamic and structural study of pyrene-1-carboxaldehyde/DNA interactions by molecular spectroscopy: Probing intercalation and binding properties, *Chem. Phys.*, 373 (2010) 186-192.
- [43] D.M. Crothers, Statistical thermodynamics of nucleic acid melting transitions with coupled binding equilibria, *Biopolymers*, 10 (1971) 2147-2160.

- [44] R. Galindo-Murillo, J.C. Robertson, M. Zgarbova, J. Sponer, M. Otyepka, P. Jurecka, T.E. Cheatham, Assessing the Current State of Amber Force Field Modifications for DNA, *J. Chem. Theory Comput.*, 12 (2016) 4114-4127.
- [45] V. Bar-Ad, J. Palmer, H.S. Yang, D. Cognetti, J. Curry, A. Luginbuhl, M. Tuluc, B. Campling, R. Axelrod, Current Management of Locally Advanced Head and Neck Cancer: The Combination of Chemotherapy With Locoregional Treatments, *Semin. Oncol.*, 41 (2014) 798-806.
- [46] L. Bussmann, C.J. Busch, B.B. Lorincz, T. Rieckmann, A. Block, R. Knecht, Perspectives in chemosensitivity and chemoresistance assays and their implementation in head and neck cancer, *Eur. Arch. Otorhinolaryngol.*, 273 (2016) 4073-4080.
- [47] D.J. Creighton, J. Hajdu, D. Sigman, Model dehydrogenase reactions. Zinc ion catalyzed reduction of chelating aldehydes by N-propyl-1,4-dihyronicotinamides and borohydride, *J. Am. Chem. Soc.*, 98 (1976) 4619-4625.
- [48] A. Ramirez-Monroy, T.M. Swager, Metal Chelates Based on Isoxazoline[60]fullerenes, *Organometallics*, 30 (2011) 2464-2467.
- [49] K. Bhadra, M. Maiti, G.S. Kumar, Molecular recognition of DNA by small molecules: AT base pair specific intercalative binding of cytotoxic plant alkaloid palmatine, *Biochimica Et Biophysica Acta-General Subjects*, 1770 (2007) 1071-1080.
- [50] M. Islam, R. Sinha, G.S. Kumar, RNA binding small molecules: Studies on t-RNA binding by cytotoxic plant alkaloids berberine, palmatine and the comparison to ethidium, *Biophys. Chem.*, 125 (2007) 508-520.
- [51] E. Krieger, G. Vriend, YASARA View-molecular graphics for all devices-from smartphones to workstations, *Bioinformatics*, 30 (2014) 2981-2982.
- [52] G.M. Morris, R. Huey, W. Lindstrom, M.F. Sanner, R.K. Belew, D.S. Goodsell, A.J. Olson, AutoDock4 and AutoDockTools4: Automated Docking with Selective Receptor Flexibility, *J. Comput. Chem.*, 30 (2009) 2785-2791.

ACCEPTED MANUSCRIPT